Utilizing Baseline Information in Addition to Task-Related Information in FMRI

Daniel B. Rowe[1,2]
[1]Department of Mathematical and Statistical Sciences, Marquette University
Milwaukee, Wisconsin, 53022
[2]Department of Biophysics, Medical College of Wisconsin
Milwaukee, Wisconsin, 53226

Abstract

The practice in fMRI brain imaging to determine brain activation within a voxel has been to detect a task-related increase in the BOLD signal from baseline. Valuable information about the tissue type contained in a voxel can be found within the baseline of the same data. Different tissue types like gray matter and white matter have different baseline intensity values. It is well known that neurons are in grey matter and thus activation should be in gray matter. This work utilizes both baseline signal and differential signal changes to determine brain activation.

Key Words: fMRI, activation, brain imaging, MRI

1. Introduction

In fMRI, a subject is placed in the MRI machine and volume images of their brain is produced at n time points while they are generally performing an experimentally designed cognitive task. In the early 1990's, fMRI (functional magnetic resonance imaging) was developed as a technique to noninvasively observe the human brain in action without exogenous contrast agents (1). FMRI is based upon the BOLD (blood oxygen level dependent contrast) in which blood oxygenation changes in the local vicinity of firing neurons (2). The practice in fMRI brain imaging is to determine brain activation within a voxel by way of a statistically significant increase in the BOLD signal.

Typically, a general linear model is fit to each voxel time series with the independent variable being the expected voxel response from the experimental stimulus paradigm. From this general linear model, every voxel has an estimate of the contribution from the stimulus β_1 along with a corresponding t-statistic describing the significance of activation (nonrandom change from baseline) within it. The t-statistics are thresholded (3,4) to separate true (biological) activation signal from noise (random variation/signal not of interest). Voxels with t-statistics above this threshold are color coded and superimposed upon a gray scale anatomical image to visualize their physical location.

However, it may be difficult to determine a useful threshold (3,4). If this threshold is determined to be too low, there are often many voxels retained that visually appear to be noise and not of biological origin. If this threshold is determined to be too low, then noise is eliminated, but true biologically active voxels may also be eliminated. From the general linear model, we also have an estimate of the baseline intensity level β_0. We can have two voxels that have the same activation level β_1 but different baselines β_0. It is well-known in fMRI that active voxels should be in gray matter and that in T_2* weighted images gray matter voxels have higher β_0 baseline intensity levels. For this reason, the baseline voxel intensity level will be useful in determining voxels that are active or statistically significantly related to the expected task response and contains grey matter within the voxel as indicated by β_0. Hence the need to utilize both β_1 and β_0 along their *t*-distribution significance levels for significance.

2. FMRI Data

In each voxel, we observe n, data points, $(x_1,y_1),\ldots,(x_n,y_n)$ and determine a statistically significant relationship between x (task design) an y (observed voxel value) as

$$y_t = \beta_0 + \beta_1 x_t + \varepsilon_t , \qquad [1]$$

where the errors have been specified to be independent normally distributed with a mean of zero and constant variance, $\varepsilon_t \sim N(0,\sigma^2)$ for $t=1,\ldots,n$. In each voxel, regression coefficients of Equation 1 are estimated as

$$\hat{\beta} = (X'X)^{-1}X'y . \qquad [2]$$

In Equation 2, X is the $n \times q$ design matrix with first column of ones and second column of the dependent variable x_t values, y is a column vector of the independent variable y_t values, and $\hat{\beta}$ is a 2×1 vector containing the estimated baseline (y-intercept) and activation (slope) coefficients.

The practice in fMRI brain imaging is to determine brain activation within a voxel by way of a statistically significant increase in the BOLD signal from baseline using Equation 3. The *t*-statistic for the activation coefficient is computed,

$$t_1 = \frac{\hat{\beta}_1}{SE(\hat{\beta}_1)} \qquad [3]$$

where $SE(\hat{\beta}) = s\sqrt{w_{22}}$ and $W=(X'X)^{-1}=[w_{11},w_{12};w_{21},w_{22}]$. Similarly, a *t*-statistic for β_0, t_0 can also be calculated.

Data from a technology development experimental fMRI study (5) that records a unilateral right-hand finger tapping task is used to demonstrate this new research. For the study, a 3.0 T General Electric Signa LX MRI scanner was utilized. The experimental data consists of n_z=7 axial slices as illustrated in Figure 1 (left) that were 2.5 mm thick, the field-of-view (FOV) was 240 mm, with the phase encoding direction oriented as posterior to anterior, flip angle of 90° and an acquisition bandwidth of 125 kHz. Each slice is an n_y=96 by n_x=96 array and there were n_t=510 volume images or time points in each voxel.

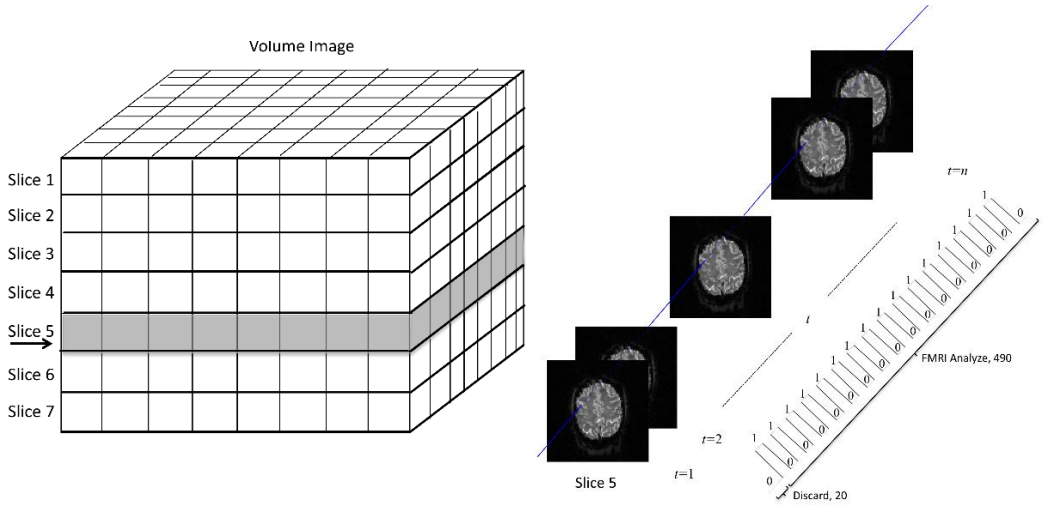

Figure 1: Illustration of single n_z=7 axial slice volume image (left) and a series of images for slice 5 (right) with task timing.

As part of this particular scan and not part of the fMRI experiment, the first 20 images varied echo time without task. Images 1-10 were at a constant echo time of 42.7 ms, images 11-15 had an echo time of 42.7 ms, 45.2 ms, 47.7 ms, 50.2 me, and 52.7, images 16-20 repeated the same echo times as images 11-15. The fMRI experimental portion of the scan consisting of the last n=490 images had a constant echo time of 42.7 ms. The fMRI experiment was a unilateral right-hand finger-tapping task in a block design with task timing displayed in Figure 1 (right) consisting of 16 epochs with 15 s off and 15 s on then a final 10 images of off with a time to repetition (TR) of 1 s. For each slice, the images are collected together as in Figure 1 (right) and the n time points for each voxel statistically analyzed. It should be noted that for these T_2* weighted images, voxels containing grey matter are brighter than those containing white matter.

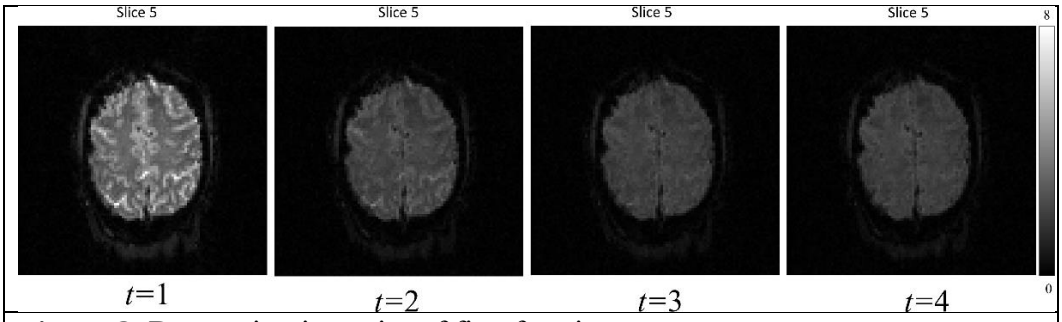

Figure 2. Decreasing intensity of first four images.

First, to explore the data, the first four images for slice 5 are presented in Figure 2. In Figure 2 we can see that the image intensity is high in the first image and decreases to equilibrium by image four. It should be noted that in nearly all fMRI studies the first few images are omitted from analysis and view by the analyst (5). Since image one is very bright and aligned with the remaining images, it will be used as an anatomical reference that statistics are superimposed upon. To continue the exploration of the data, a mask is generated. To form these masks the voxels for the fMRI experiment were time averaged to reduce noise and a histogram of the $n_x n_y n_z$=64512 time averaged voxel intensities presented in Figure 3. Note that in Figure 3 we can clearly see one population of intensities for voxels outside the brain with a Rice-like distribution and another population of voxels inside the brain with a normal-like distribution. These averaged images were subsequently smoothed with 5×5 mean filter, then pixel intensities larger than one were designated to be within the brain set to 1 while the remaining voxels were designated outside the brain and set to 0 and. These masks presented in Figure 4 are to be used to examine voxel statistics inside and outside the brain.

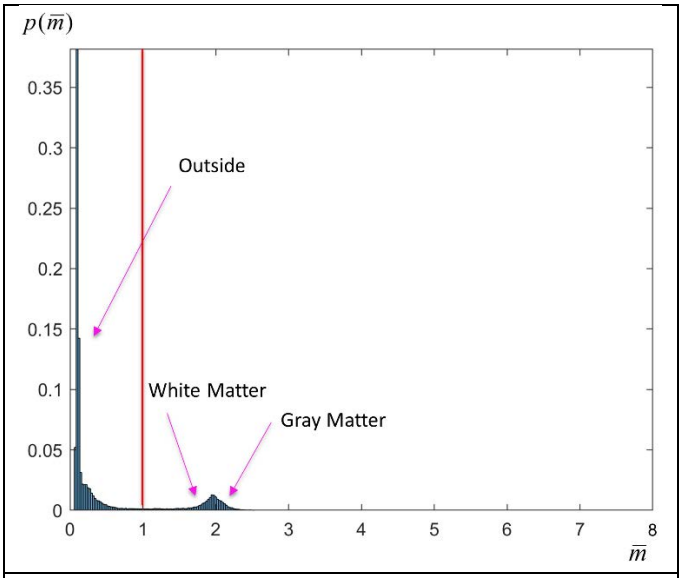

Figure 3. Histogram of averaged pixel intensities.

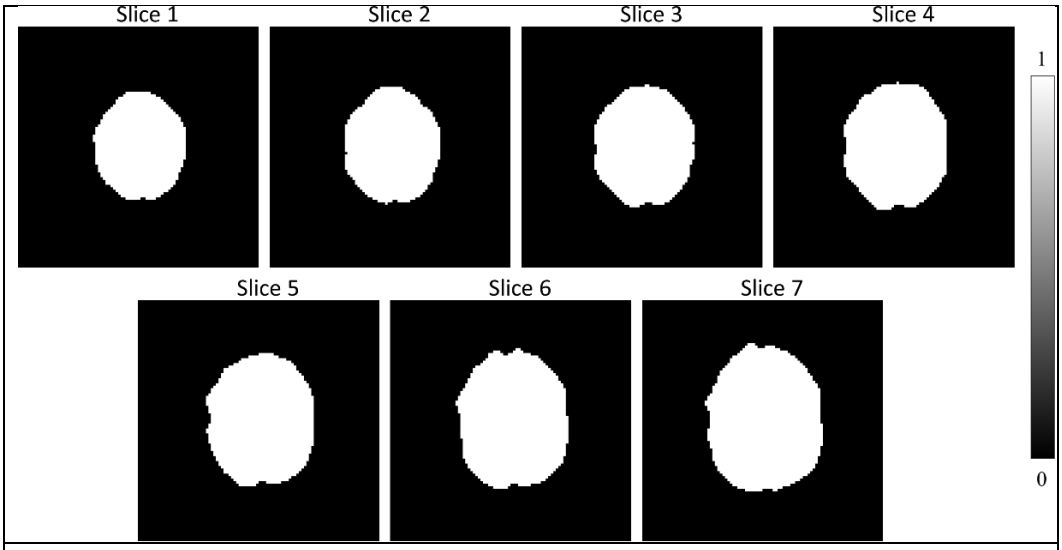

Figure 4. Spatial masks delineating inside and outside brain voxels.

Now that we have these spatial masks, histograms can be made. The first scan images for the slices that are used as our anatomical reference is presented in Figure 5.

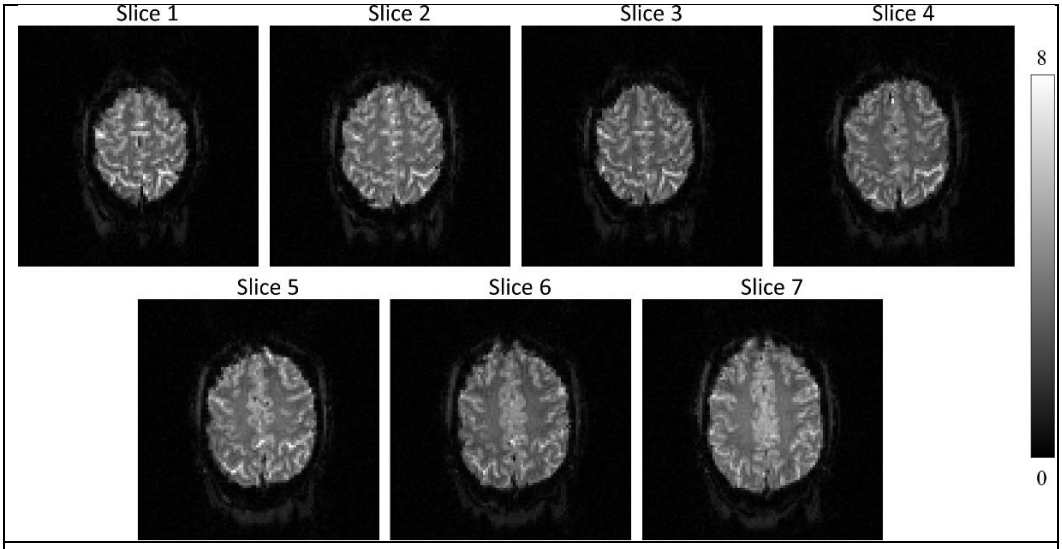

Figure 5. First scan (t=21) image for the n=7 slices.

Upon utilizing the mask in Figure 4 on the anatomical images in Figure 5 we obtain the histograms in Figure 6 of the $n_x n_y n_z$=64512 voxel values. Voxels outside the brain mask are colored red and those inside the brain colored blue. Again, in Figure 6, note the Rice-like distribution for voxels outside the brain and normal-like distribution of voxels inside the brain. It should be noted that the population considered outside the brain contains voxels with some signal in them presumably warped pixels of skin and adipose tissue as seen in Figure 5.

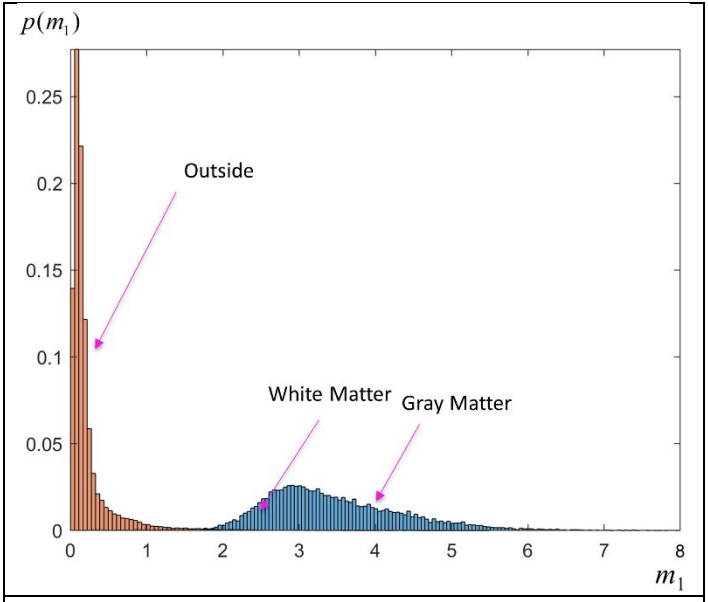

Figure 6. Histogram of anatomical images.

To examine fMRI experiment voxels, the mask was applied to the n=490 images of the n_z=7 slices. The first fMRI experimental time point images are presented in Figure 7. The remaining experimental images are not visually different other than minor noise. Note that the slice 5 image in Figure 7 appear visually similar to the slice t=4 discarded image in Figure 2 indicating that the first fMRI image intensities have equilibrated.

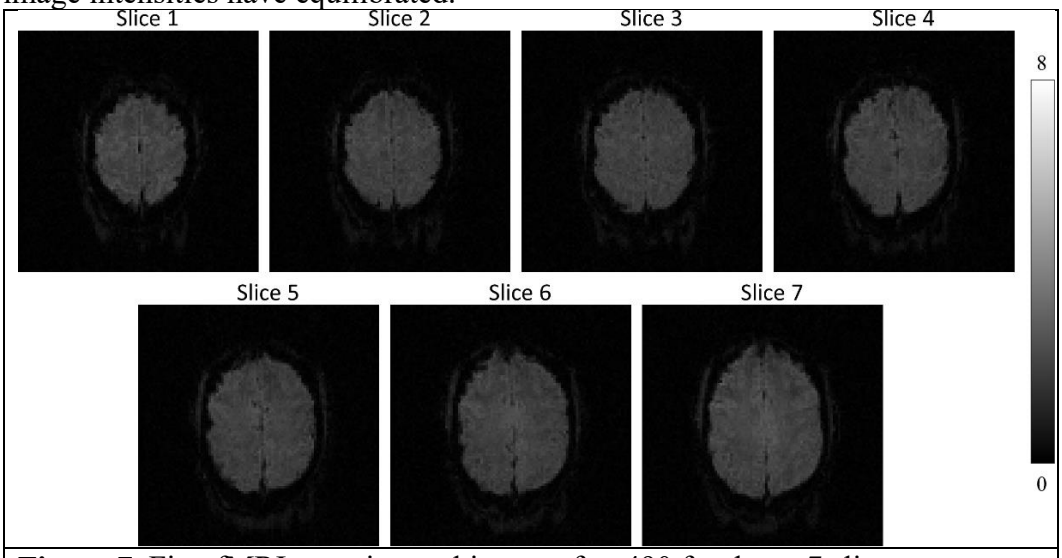

Figure 7. First fMRI experimental image of n=490 for the n=7 slices.

Upon utilizing the mask in Figure 4 on the functional images in Figure 7 we obtain the histograms in Figure 8 of the $n_x n_y n_z n$=31610880 voxel values. Voxels outside the brain mask are colored red and those inside the brain colored blue. Again, in Figure 6, note the Rice-like distribution for voxels outside the brain and normal-like distribution of voxels inside the brain. It should be noted that the population considered outside the brain again contains voxels with some signal in them presumably warped pixels as seen in Figure 7.

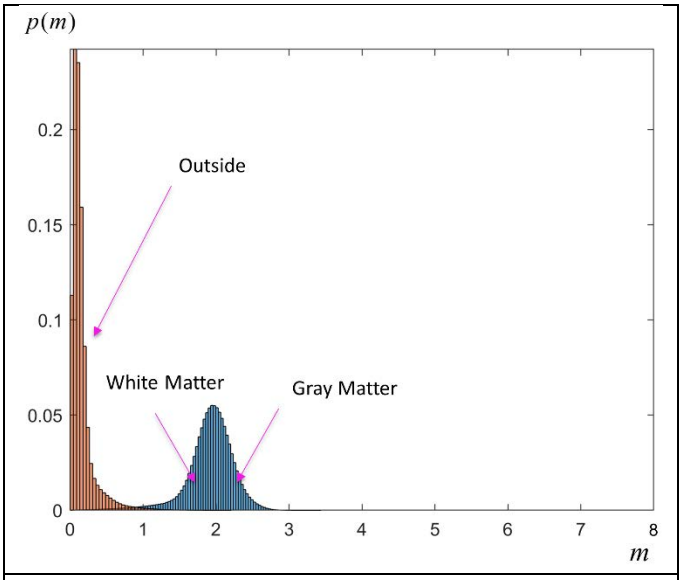

Figure 8. Histogram of functional images.

3. Differential Activation

To examine results of the standard fMRI experiment analysis, a linear regression model was fit to the n=490 time points in each voxel. This linear regression model as in Equation 1 contained a design matrix with first column of ones and second column of zeros and ones following the previously described design but shifted forward by four time points to account for the hemodynamic delay. Figure 9 presents the $\hat{\beta}_0$ coefficients of every voxel.

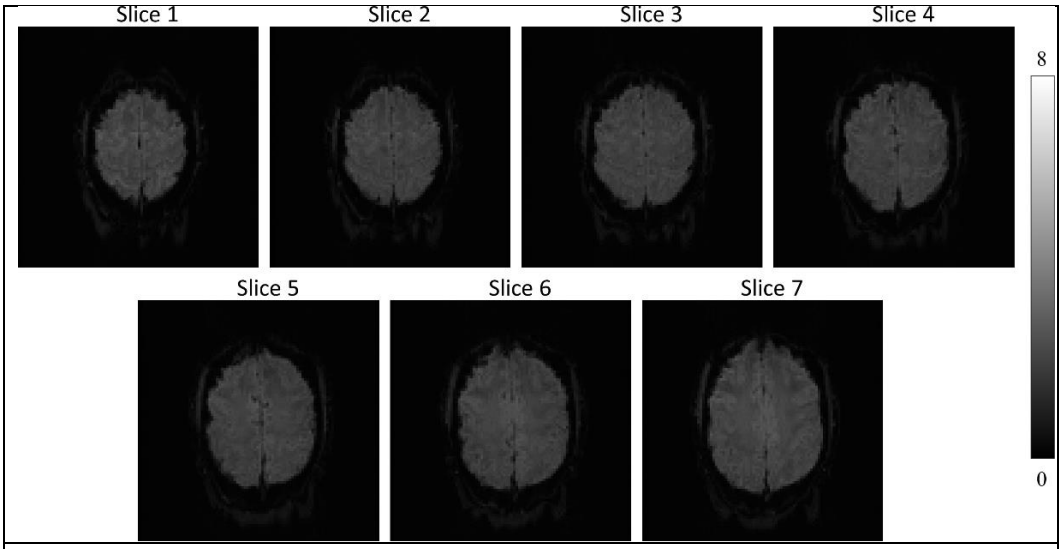

Figure 9. Maps of baseline $\hat{\beta}_0$ coefficients for the n=7 slices.

Upon utilizing the mask in Figure 4 on the functional images in Figure 9 we obtain the histograms in Figure 10 of the $n_x n_y n_z$=64512 voxel baseline (y-intercept) values. Voxels outside the brain mask are colored red and those inside the brain colored blue. Again, in Figure 10, note the Rice-like distribution for voxels outside the brain and normal-like distribution of voxels inside the brain. It should be noted that the population considered outside the brain again contains voxels with some signal in them presumably warped pixels as seen in Figure 9.

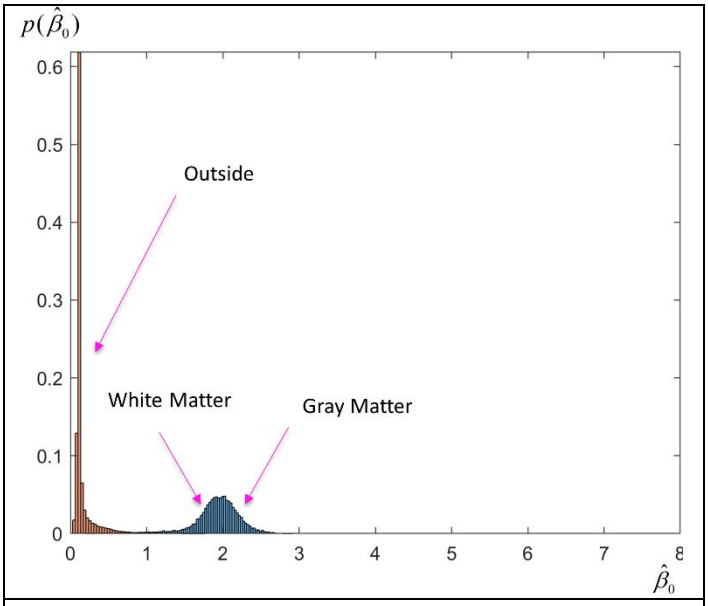

Figure 10. Histogram of $\hat{\beta}_0$ coefficients.

Now that we have examined the properties of voxels both inside and outside the brain, we can now focus on the voxels within the brain which are of primary interest. The voxels outside the brain were omitted and the $\hat{\beta}_0$ voxels within the brain represented on a narrower limit and colored as in Figure 11.

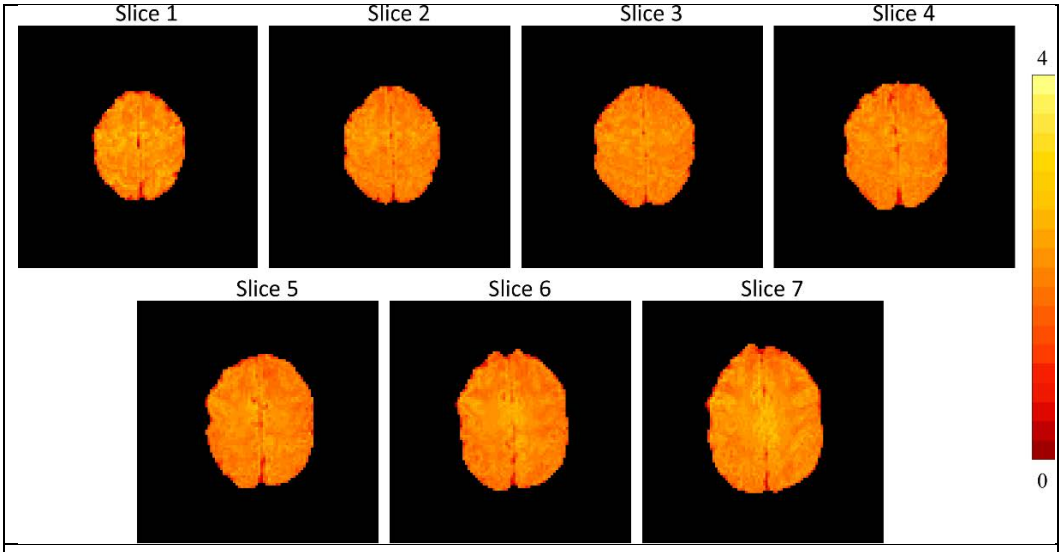

Figure 11. Maps of baseline $\hat{\beta}_0$ coefficients for the n=7 slices.

Upon utilizing the mask in Figure 4 on the $\hat{\beta}_0$ coefficients in Figure 9 we obtain the histogram in Figure 12 of the 11792 within brain $\hat{\beta}_0$ coefficients. In Figure 12, note the normal-like distribution of voxels inside the brain but with a longer tail to the left. It is possible that these lower $\hat{\beta}_0$ coefficients are within the brain cerebral spinal fluid (CSF) voxels or voxels from the mask extending slightly outside the brain.

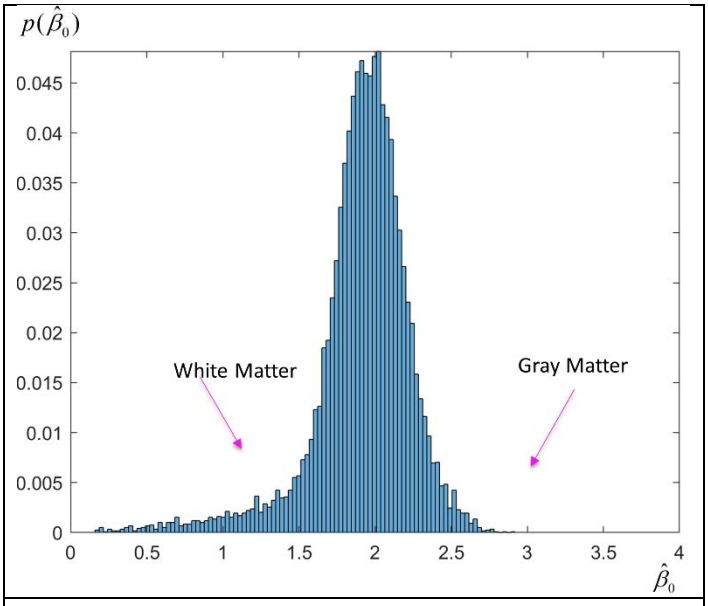

Figure 12. Histogram of $\hat{\beta}_0$ coefficients.

We can also examine the $\hat{\beta}_1$ coefficients within the brain as shown in Figure 13. As expected from the unilateral finger tapping task, there are large task-related coefficients in the left motor cortex in most slices and in the supplementary motor area (SMA) activation in slices 4 and 5. Every voxel within the brain has a *t*-statistic associated with the task displayed.

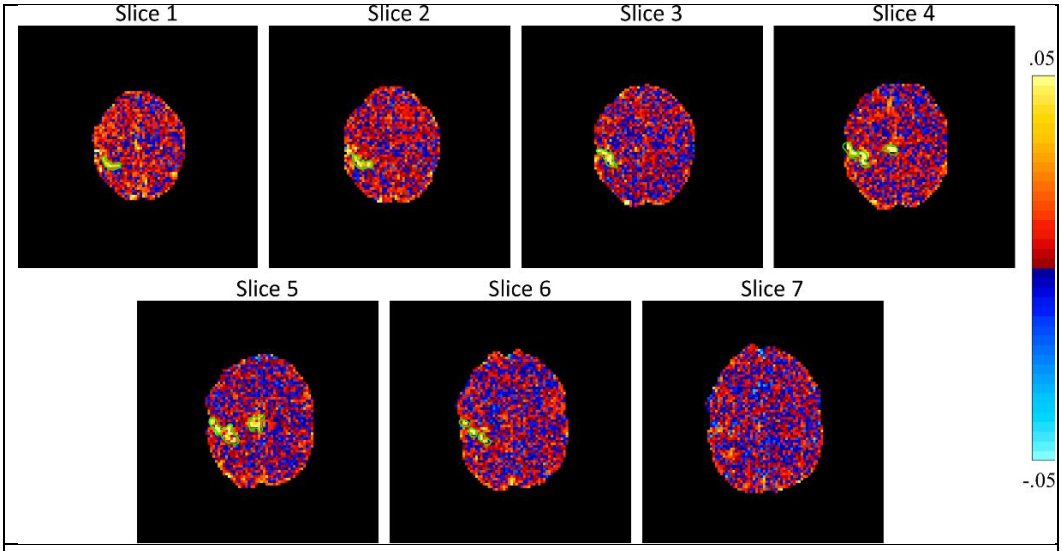

Figure 13. Maps of task $\hat{\beta}_1$ coefficients for the n=7 slices.

We obtain the histogram in Figure 14 of the 11792 within brain $\hat{\beta}_1$ coefficients. In Figure 14, note the normal-like distribution of voxels inside the brain centered at zero but with a marginally longer tail to the right. This histogram contains grey matter, white matter, and CSF voxels. The $\hat{\beta}_1$ statistics in the upper tail appear to be the ones from task active voxels outlined in green.

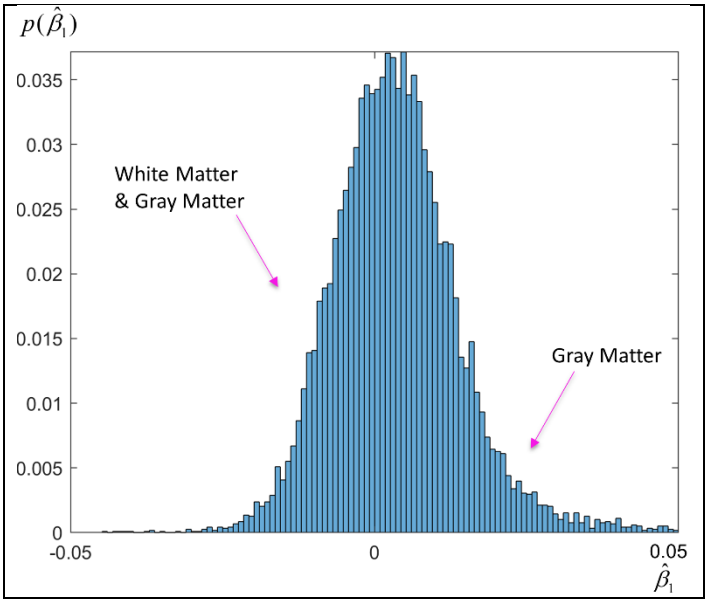

Figure 14. Histogram of $\hat{\beta}_1$ coefficients.

The task related $\hat{\beta}_1$ regression coefficients can be converted into *t*-statistics using Equation 3, denoted as t_1. And displayed in Figure 15. As expected from the unilateral finger tapping task, there is high activation in the left motor cortex in most slices and in the supplementary motor area activation in slices 4 and 5. Every voxel within the brain has a *t*-statistic associated with the task displayed. The usual practice is to only consider these t_1 statistics when determining which voxels are considered active. Many thresholding procedures can be applied including ones that consider clusters sizes voxels. Note the same delineation of the left motor cortex and SMA areas within the green regions.

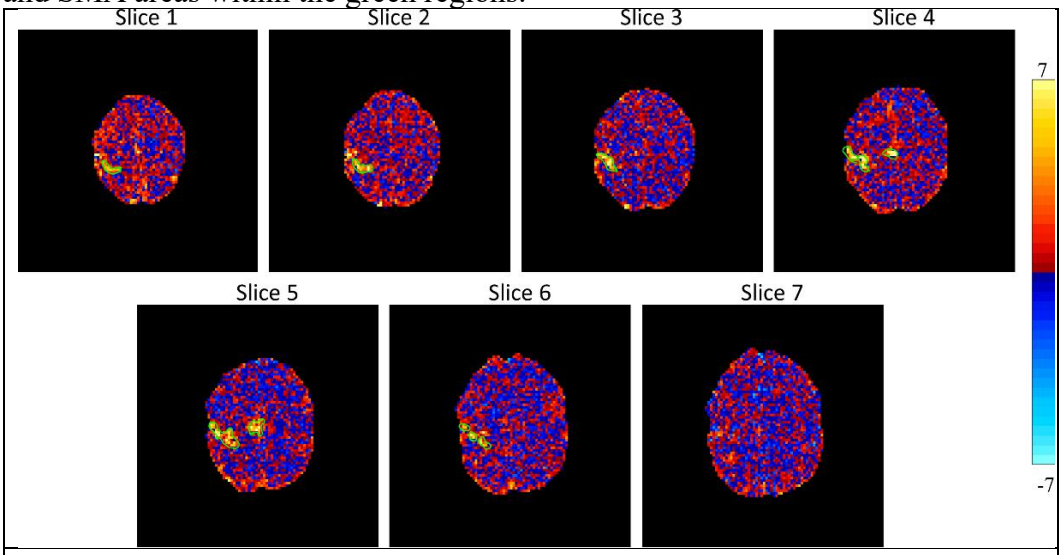

Figure 15. Maps of task t_1 coefficients for the n=7 slices.

A histogram of these t_1 statistics can be made as shown in Figure 16. In Figure 16, note the normal-like distribution of voxels inside the brain centered at zero but with a marginally longer tail to the right. The t_1 statistics in the upper tail are the ones that are task active according to the standard activation procedure. In Figure 16 a red vertical line is presented where $t_{.05}$=1.645 indicating a potential threshold.

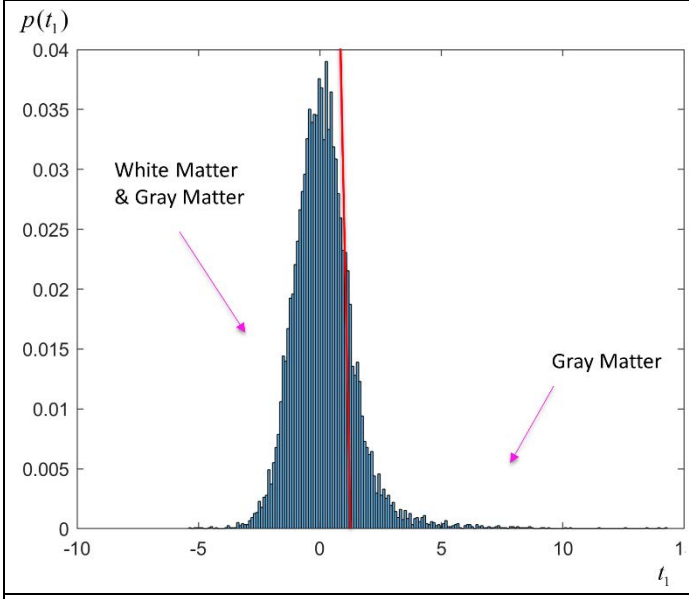

Figure 16. Histogram of $\hat{\beta}_1$ coefficients.

To examine the typical activation technique, a threshold of $t_{.05}$=1.645 was applied to the within brain activation statistics. These thresholded activation statistics are presented in Figure 17. Although it appears that the active voxels in the left motor cortex and SMA are discovered, they are obfuscated by the many false positive noise activations. Raising this threshold would eliminate the false positives, but may also remove the true positives. As previously noted, the goal of this research is to utilize information that may be contained in the $\hat{\beta}_0$ coefficients or their associated t_0 statistics.

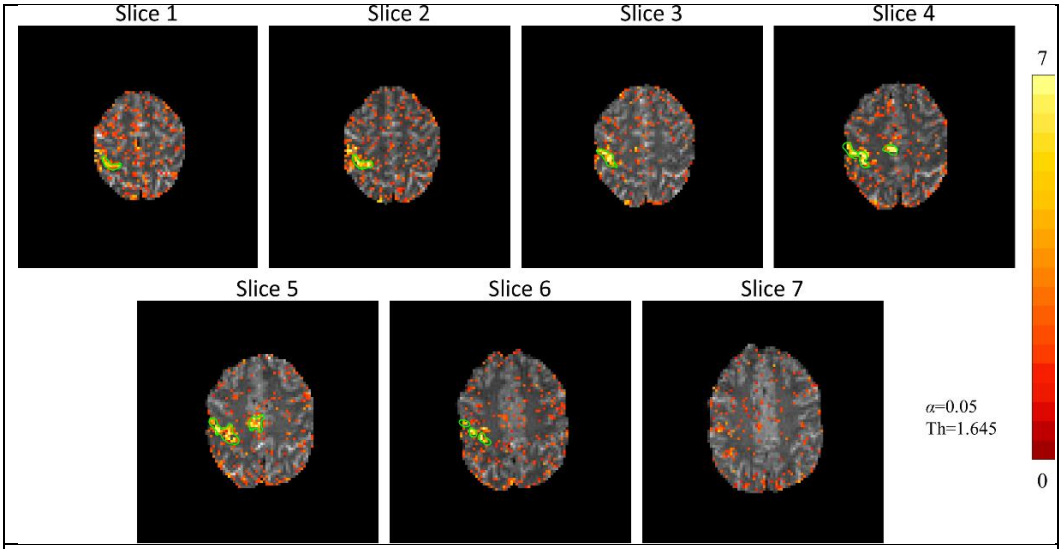

Figure 17. Maps of thresholded task t_1 coefficients for the n=7 slices.

The baseline $\hat{\beta}_0$ regression coefficients were converted into *t*-statistics denoted as t_0 and displayed in Figure 18. The t_0 statistics appear to be larger in grey matter than in white matter.

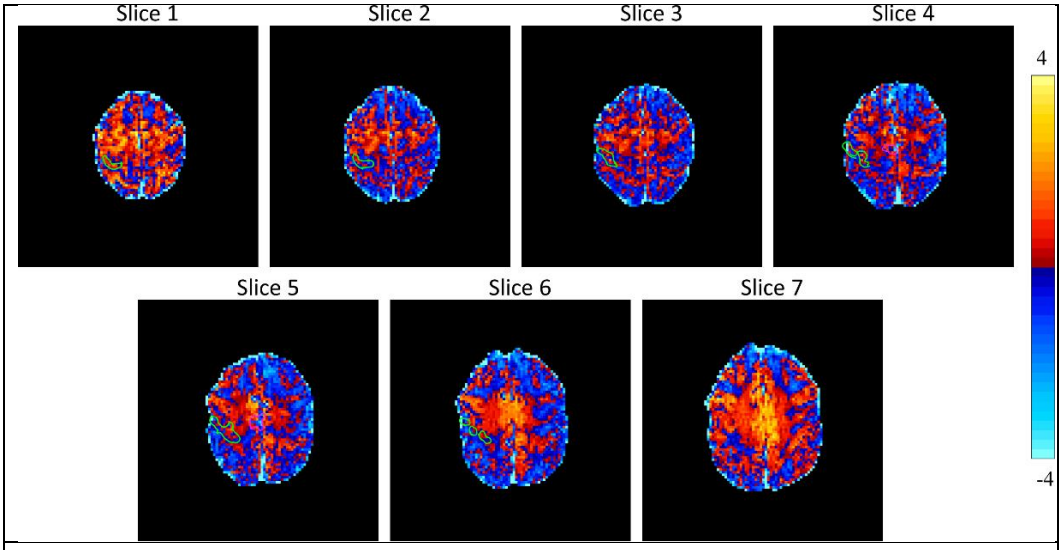

Figure 18. Maps of task $\hat{\beta}_0$ coefficients for the n=7 slices.

The larger t_0 statistics in grey matter indicates that there is information in them to assist in delineating grey matter versus white matter voxels.

It is believed by neuroscientists that activation should occur in grey matter voxels. A histogram of these 11792 within brain t_0 statistics can be made as shown in Figure 19. In Figure 19, note the normal-like distribution of voxels inside the brain centered at zero but with a marginally longer tail to the left. It is possible that these lower t_0 coefficients are within the brain cerebral spinal fluid (CSF) voxels or voxels from the mask extending slightly outside the brain.

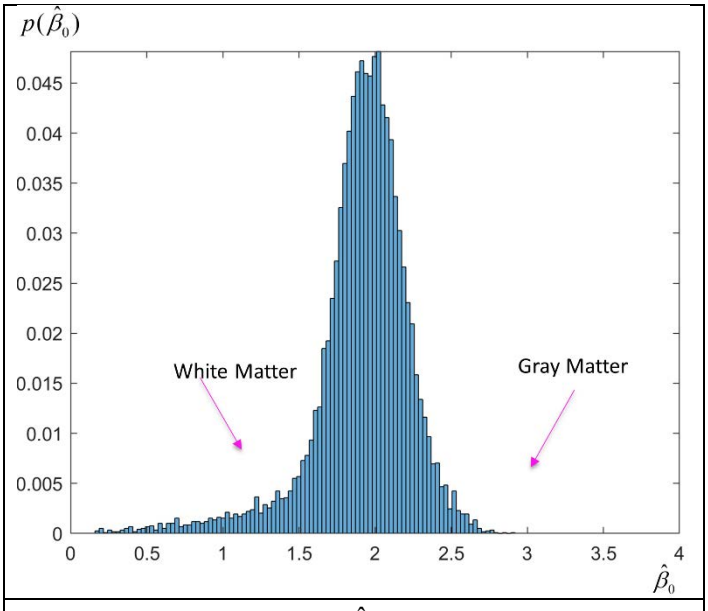

Figure 19. Histogram of $\hat{\beta}_0$ coefficients.

4. Baseline Information

The rational for this study is that we can utilize information in both $\hat{\beta}_0$ and $\hat{\beta}_1$ to determine which voxels in grey matter are active. Focusing on slice 5 and applying a mild t_{thresh}=1.645 threshold to the differential t_1-statistics, we see meaningful brain activation but with many false positives. Figure 20 highlights two voxels with similar activation t_1 statistics around 3.7 but drastically different baseline $\hat{\beta}_0$ statistics.

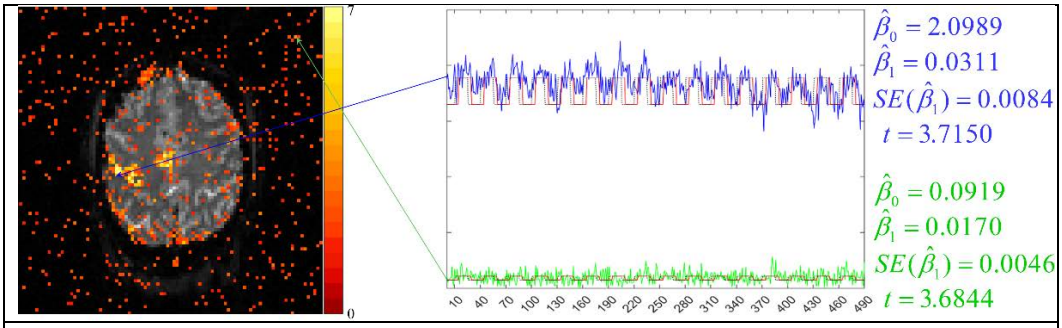

Figure 20: Two similarly active voxels with different baselines.

These two voxels give us motivation to use information contained in $\hat{\beta}_0$. Ideally, we would like to declare voxels active that have large t_1 statistics and also large t_0 statistics.

For voxels inside the brain, a bivariate plot of the $\hat{\beta}_0$ and $\hat{\beta}_1$ statistics was made as seen in Figure 21. With the use of Matlab, a two population gaussian mixture model was fit to the coefficients in Figure 21. It is evident that we would like to have active voxels that are in the upper right area of the bivariate distribution.

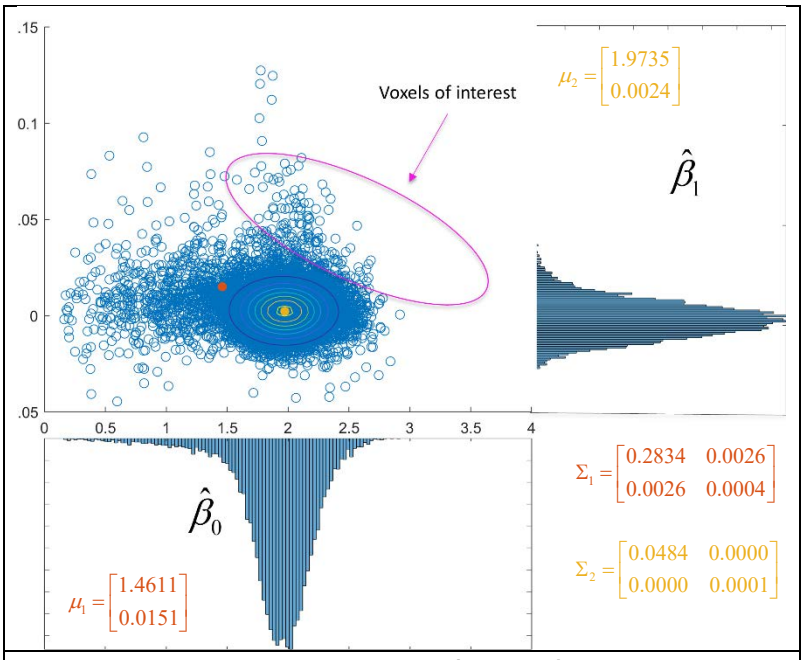

Figure 21: Bivariate plot of the $\hat{\beta}_0$ and $\hat{\beta}_1$ statistics.

We would also like to take into account random variation of each coefficient by converting them to *t*-statistics.

The $\hat{\beta}_0$ and $\hat{\beta}_1$ regression coefficients in Figure 22 were converted into *t*-statistics. The bivariate mixture model mean of 1.4611 was subtracted from the estimated $\hat{\beta}_0$ coefficient and divided by its standard error *SE*($\hat{\beta}_0$) to form t_0's. The hypothesized mean of 0 was subtracted from each voxel's $\hat{\beta}_1$ and divided by its standard error *SE*($\hat{\beta}_1$) to form t_1's.

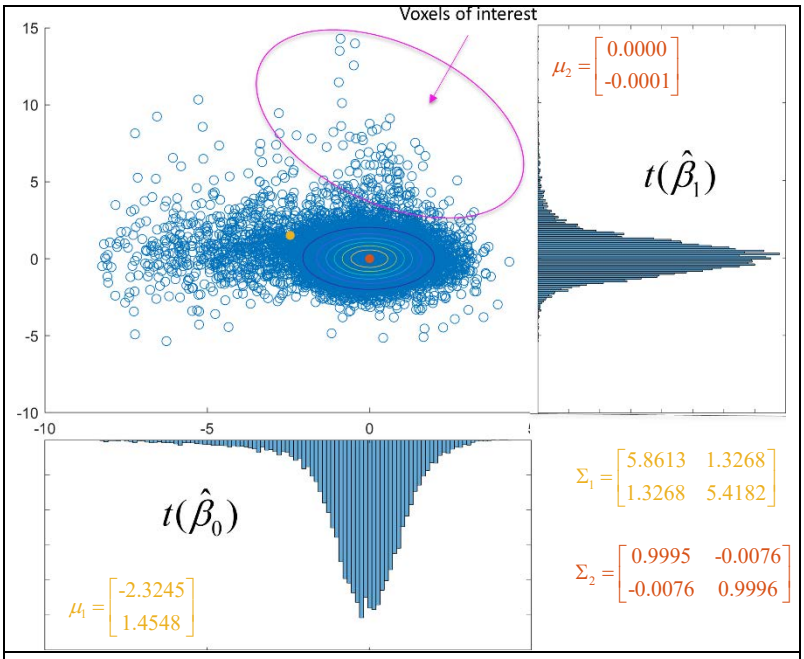

Figure 22: Bivariate plot of the t_0 and t_1 statistics.

It is clear in Figure 22 that we would like to retain voxels that are in the upper right quadrant of the bivariate distribution. To utilize the *t*-statistic *p*-values in a bivariate way, the *p*-values p_0 and p_1 corresponding to t_0 and t_1 were multiplied together. Since it is difficult to visually see a broad range of probabilities their negative logarithm, $-log_{10}(p_0p_1)$ was taken. A map of these negative log base 10 product *p*-values is presented in Figure 23. Note the same delineation of the left motor cortex and SMA areas within the green regions.

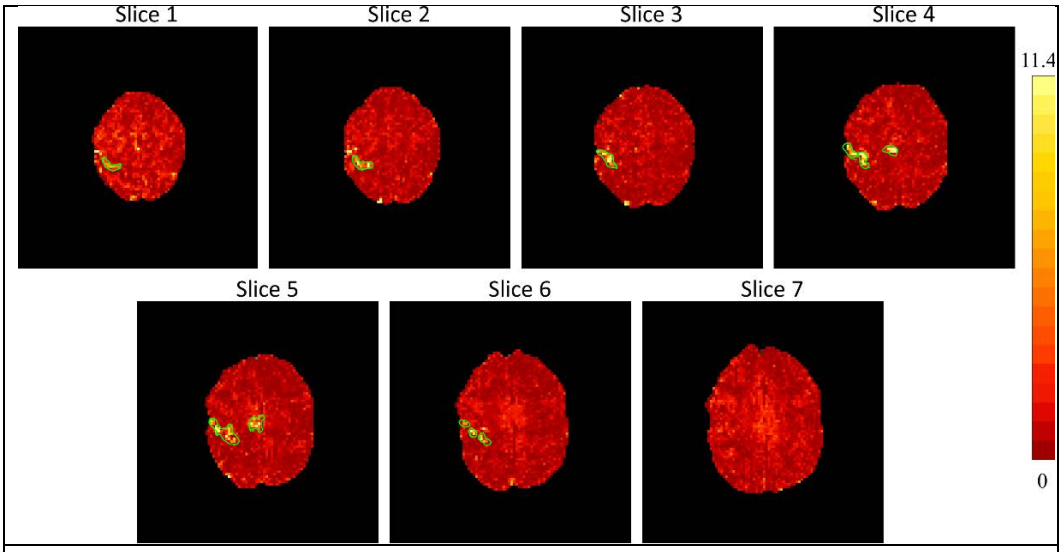

Figure 23. Maps of task -$log_{10}(p_0p_1)$ statistics for the n=7 slices.

The statistic values in Figure 23 were thresholded at the -$log_{10}(p_0p_1)$ =5 (p_0=0.01 and p_1=0.01). These negative log base 10 product p-values are presented in Figure 24. Note that there are far fewer false positives.

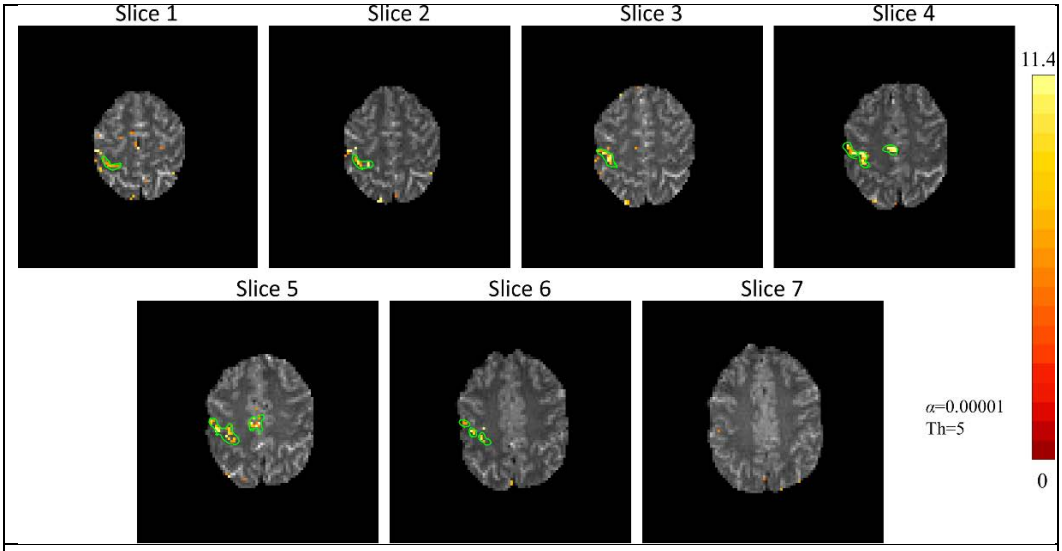

Figure 24. Maps of thresholded task -$log_{10}(p_0p_1)$ statistics for the n=7 slices.

5. Discussion

The usual MRI process with t-statistics of β_1 was presented. The usually discarded first images data was presented. The usual β_0 and of β_1 coefficients were presented as parametric maps as were their t-statistics. Baseline anatomical information was explored along with differential functional information to determine brain activation. Utilizing the baseline signal intensity which is a strong indicator of tissue type can assist in detecting activation in gray matter tissue and

reduce false positives. The bivariate distribution of β_0 and of β_1 were presented as were the bivariate distributions of their *t*-statistics. Presented new *t*-statistics of β_0 and of β_1. Presented way to bivariate threshold on β_0 and of β_1. By utilizing *t*-statistics for differential activation along with baseline intensity level, more accurate activation maps with less noise and improved interpretability can be derived.

References

1. Bandettini P, Jesmanowicz A, Wong E, Hyde JS. Processing strategies for time-course data sets in functional MRI of the human brain. Magn Reson Med 30:161–173, 1993.
2. Ogawa S, Lee TM, Nayak AS, Glynn P. Oxygenation-sensitive contrast in magnetic resonance image of rodent brain at high magnetic fields. Magn Reson Med 14(1):68–78, 1990.
3. Logan BR, Rowe DB. An evaluation of thresholding techniques in fMRI analysis. Neuroimage 22(1):95–108, 2004.
4. Logan BR, Geliazkova MP, Rowe DB. An evaluation of spatial thresholding techniques in fMRI analysis. Hum Brain Mapp 29(12):1379–1389, 2008.
5. Karaman MM, Bruce IP, Rowe DB: A statistical fMRI model for differential T_2* contrast incorporating T_1 and T_2* of gray matter. Magn Reson Imaging, 32(1):9–27, 2014.